affinity. In contrast, *meso*-Fe(EHPG)$^-$, which has one equatorial and one axial phenolate, has much lower affinity for HSA. We suggest that, in the case of these unsubstituted derivatives with relatively low binding affinity, the overall shape of the complexes is as important as various individual contributions to the binding free energy (hydrogen bonds, van der Waals interactions, etc.). Thus, while the structures of Fe(HBED)$^-$ and *rac*-Fe(EHPG)$^-$ are quite different in some respects (e.g., the twist of the phenolate rings, the placement of carboxylate groups, and the presence of secondary nitrogens), the extended, cylindrical shape of the molecules apparently leads to similar binding activity, perhaps at a cleftlike site on the protein surface. Our studies indicate that the high-affinity bilirubin site on HSA is a likely candidate.

The binding of the chelates to HSA increases their relaxivity substantially. These coordinatively saturated complexes most likely relax water protons via transient hydrogen bonds from solvation waters.[1,6b] The observed enhancement in outer-sphere (or second-coordination-sphere) relaxivity is consistent with the binding of the chelates on the surface of HSA wherein a portion of the solvation layer of the chelate would be expected to persist.

Acknowledgment. This work was supported by PHS Grant Nos. GM37777, awarded by the National Institute of General Medical Sciences, and CA42430, awarded by the National Cancer Institute. We thank Dr. William M. Davis and the X-ray diffraction facility at the Massachusetts Institute of Technology Department of Chemistry for cooperation in this project.

Supplementary Material Available: Listings of calculated coordinates and B(eq) parameters of hydrogen atoms (Table V) and anisotropic thermal parameters for all non-hydrogen atoms (Table VI) (4 pages); a listing of final observed and calculated structure factors (Table VII) (39 pages). Ordering information is given on any current masthead page.

Contribution from the Laboratoire de Cristallographie et de Physique Cristalline (URA 144, CNRS), Université de Bordeaux I, 33405 Talence, France, and Laboratoire de Chimie Inorganique (URA 420, CNRS), Université de Paris-Sud, 91405 Orsay, France

Structural Changes Associated with the Spin Transition in $Fe(phen)_2(NCS)_2$: A Single-Crystal X-ray Investigation

Bernard Gallois,*[1a] José-Antonio Real,[1b,c] Christian Hauw,[1a] and Jacqueline Zarembowitch*[1b]

Received May 24, 1989

The crystal structure of $Fe(phen)_2(NCS)_2$ (phen = 1,10-phenanthroline) was determined by X-ray diffraction at ≈293 and ≈130 K, in order to detect the structural changes associated with the singlet ↔ quintet spin transition. The space group is *Pbcn* with $Z = 4$ at both temperatures. Lattice constants are as follows: $a = 13.1612$ (18), $b = 10.1633$ (11), and $c = 17.4806$ (19) Å at ≈293 K and $a = 12.7699$ (21), $b = 10.0904$ (25), and $c = 17.2218$ (30) Å at ≈130 K. The data were refined (167 parameters) to $R = 3.4\%$ (4.1%) at ≈293 K (≈130 K) for 1050 (1115) observed independent reflections ($F_o^2 > 2\sigma(F_o)^2$). In disagreement with most of the predictions, the transition is found to be accompanied neither by a change in the crystal symmetry nor by an order–disorder transition involving $(NCS)^-$ groups. Only a large reorganization of the iron(II) environment is detected. The main structural modifications, when passing from the high- to the low-spin form, consist of an important shortening of the Fe–N(phen) and Fe–N(CS) distances (by 0.20 (mean value) and 0.10 Å, respectively) and a noticeable variation of the N–Fe–N angles, leading to a more regular shape of the [Fe–N_6] octahedron. The temperature dependence of $\chi_m T$ (χ_m = molar magnetic susceptibility), determined on a polycrystalline sample of $Fe(phen)_2(NCS)_2$, shows the existence of a sharp transition centered at $T_c \approx 176.5$ K. The higher and lower limits of $\chi_m T$ (3.41 and 0.58 $cm^3 \cdot mol^{-1} \cdot K$) indicate that the compound is in the high-spin state at room temperature, whereas ≈17% of the high-spin isomer is retained in the low-spin form at low temperature. On account of this magnetic behavior and of the crystallographic data, the compound is assumed to be in the crystalline form "II", by analogy with $Fe(bpy)_2(NCS)_2$ (bpy = 2,2′-bipyridine).

Introduction

The compound *cis*-bis(thiocyanato)bis(1,10-phenanthroline)-iron(II), $Fe(phen)_2(NCS)_2$, has been known since the 1960s[2-5] to exhibit a discontinuous $S = 2 \leftrightarrow S = 0$ spin crossover in the solid state, at a critical temperature T_c close to 176 K.

This complex is one of the spin-crossover systems that have been most investigated.[6] Various techniques were used to study its transition: magnetic susceptibility measurements,[2,4,5,7-10] Mössbauer,[4,5,8,9,11,12] infrared,[3,5,12-16] and UV–visible[5] spectrometries, calorimetric measurements,[9,15,17] X-ray powder diffraction[2,4,5,9] and absorption (EXAFS, XANES, edge),[18] NMR spectrometry[11,19] and XPS.[20,21] In all the above-mentioned studies, the spin transition of $Fe(phen)_2(NCS)_2$ was thermally driven. However, this transition has also been induced by pressure,[22-25] by both pressure and temperature,[24-26] and by light irradiation (the phenomenon being called "light-induced excited spin state trapping" or LIESST).[16,27] On the other hand, among the additional investigations related to $Fe(phen)_2(NCS)_2$, let us point out the following: the influence of a magnetic field on the critical temperature value,[28] the effect of metal dilution on the transition

(1) (a) Université de Bordeaux I. (b) Université de Paris-Sud. (c) Permanent address: Departamento de Quimica Inorganica, Facultad de Farmacia, Universidad de Valencia, Valencia, Spain.
(2) Baker, W. A.; Bobonich, H. M. *Inorg. Chem.* **1964**, *3*, 1184.
(3) Baker, W. A.; Long, G. J. *Chem. Commun.* **1965**, *15*, 368.
(4) König, E.; Madeja, K. *Chem. Commun.* **1966**, *3*, 61.
(5) König, E.; Madeja, K. *Inorg. Chem.* **1967**, *6*, 48.
(6) Gütlich, P. *Struct. Bonding (Berlin)* **1981**, *44*, 83.
(7) Casey, A. T.; Isaac, F. *Aust. J. Chem.* **1967**, *20*, 2765.
(8) Ganguli, P.; Gütlich, P. *J. Phys.* **1980**, *41*, C1-313.
(9) Ganguli, P.; Gütlich, P.; Müller, E. W.; Irler, W. *J. Chem. Soc., Dalton Trans.* **1981**, 441.
(10) Müller, E. W.; Spiering, H.; Gütlich, P. *Chem. Phys. Lett.* **1982**, *93*, 567.
(11) Dézsi, I.; Molnar, B.; Tarnoczi, T.; Tompa, K. *J. Inorg. Nucl. Chem.* **1967**, *29*, 2486.
(12) Savage, S.; Jia-Long, Z.; Maddock, A. G. *J. Chem. Soc., Dalton Trans.* **1985**, 991.
(13) König, E.; Madeja, K. *Spectrochim. Acta* **1967**, *23A*, 45.
(14) (a) Takemoto, J. H.; Hutchinson, B. *Inorg. Nucl. Chem. Lett.* **1972**, *8*, 769. (b) *Inorg. Chem.* **1973**, *12*, 705.
(15) Sorai, M.; Seki, S. *J. Phys. Chem. Solids* **1974**, *35*, 555.
(16) Herber, R.; Casson, L. M. *Inorg. Chem.* **1986**, *25*, 847.
(17) Sorai, M.; Seki, S. *J. Phys. Soc. Jpn.* **1972**, *33*, 575.
(18) Cartier, C.; Thuéry, P.; Verdaguer, M.; Zarembowitch, J.; Michalowicz, A. *J. Phys.* **1986**, *47*, C8-563.
(19) Rao, P. S.; Ganguli, P.; McGarvey, B. R. *Inorg. Chem.* **1981**, *20*, 3682.
(20) Vasudevan, S.; Vasan, H. N.; Rao, C. N. R. *Chem. Phys. Lett.* **1979**, *65*, 444.
(21) Burger, K.; Furlani, C.; Mattogno, G. *J. Electron Spectrosc. Relat. Phenom.* **1980**, *21*, 249.
(22) Fischer, D. C.; Drickamer, H. G. *J. Chem. Phys.* **1971**, *54*, 4825.
(23) Ferraro, J. R.; Takemoto, J. *Appl. Spectrosc.* **1974**, *28*, 66.
(24) Adams, D. M.; Long, G. J.; Williams, A. D. *Inorg. Chem.* **1982**, *21*, 1049.
(25) Pebler, J. *Inorg. Chem.* **1983**, *22*, 4125.
(26) Usha, S.; Srinivasan, R.; Rao, C. N. R. *Chem. Phys.* **1985**, *100*, 447.
(27) Decurtins, S.; Gütlich, P.; Köhler, C. P.; Spiering, H. *J. Chem. Soc., Chem. Commun.* **1985**, 430.

0020-1669/90/1329-1152$02.50/0

characteristics,[29,30] and the analysis of the phenomenon cooperativity, on the basis of variable-temperature magnetic moment data, using a thermodynamic formulation of intermolecular interaction and lattice continuity effects.[31]

It is now well established that several characteristics of the $Fe(phen)_2(NCS)_2$ spin transition, particularly its sharpness and the fraction of high-spin residue at low temperature, strongly depend on the method of preparation of the compound. The "extraction" method, which consists in removing one molecule of 1,10-phenanthroline from $[Fe(phen)_3](NCS)_2 \cdot H_2O$ with acetone in a Soxhlet apparatus,[5] leads to a transition more abrupt and complete than the "precipitation" method, which consists of adding 1,10-phenanthroline either to $Fe(py)_4(NCS)_2$ (in pyridine, py)[5] or to $Fe(NCS)_2$ (in methanol).[9] The difference in behavior presented by "extracted" and "precipitated" samples was ascribed to differences in the size and principally in the quality of crystallites.[9,10] In both cases, the existence of a latent heat[9,15,17] and that of a thermal hysteresis (which was only detected recently on account of its narrowness[10]) suggest that the transition proceeds as a first-order transition. This is supported by the time dependence of the magnetic susceptibility observed upon the spin change,[7,9,10] which is indicative of a significant rearrangement in the solid. However, the X-ray powder spectra carried out between 295 and 80 K only exhibit small differences,[9] thus implying that the structural characteristics of the high- and low-spin phases are rather similar.

In order to get further information likely to clarify these particularities, we have attempted to obtain single crystals of $Fe(phen)_2(NCS)_2$. We report here the first single-crystal X-ray diffraction structure of both spin isomers and also the temperature dependence of the $\chi_m T$ product (χ_m = molar magnetic susceptibility) for a polycrystalline sample of the same origin as the crystal used for X-ray experiments.

Experimental Section

Growth of Single Crystals. Single crystals of $Fe(phen)_2(NCS)_2$ were obtained by the slow diffusion method, in methanol, under an argon atmosphere, using a H double-tube glass vessel. The starting materials were, on the one hand, a methanolic solution of 1,10-phenanthroline, on the other hand, the red precipitate of $Fe(pyz)_2(NCS)_2$ obtained in situ in methanol by adding pyrazine to the yellow form of $Fe(py)_4(NCS)_2$ in a 2:1 ratio. The utilization of $Fe(pyz)_2(NCS)_2$ instead of $Fe(py)_4(NCS)_2$ is justified by its slower diffusion rate in methanol. All the reagents were used in stoichiometric proportions. $Fe(py)_4(NCS)_2$ was prepared as previously described.[32] After 3 weeks, very dark crystals were collected, washed with methanol, and dried in an argon stream.

Magnetic Susceptibility Measurements. These measurements were performed on a polycrystalline sample weighing 5.20 mg, over the temperature range 295–90 K, by using a Faraday-type magnetometer equipped with an Oxford Instruments continuous-flow cryostat. The independence of the susceptibility with regard to the applied magnetic field was checked at room temperature. $HgCo(NCS)_4$ was used as a susceptibility standard. The diamagnetism correction was estimated to be 330×10^{-6} $cm^3 \cdot mol^{-1}$. The uncertainty on the temperature is about 0.1 K.

Solution and Refinement of the X-ray Structures. Preliminary X-ray investigations have been performed at ≈293 and ≈130 K by the usual photographic methods. No extra spots have been observed below the transition temperature in spite of a long exposure time. Symmetries in the diffraction patterns and systematic extinctions indicate that the space group is orthorhombic (*Pbcn*) at room temperature and does not change on cooling.

Intensity data collections were obtained at ≈293 and ≈130 K on an Enraf-Nonius CAD-4 diffractometer with monochromatized Mo Kα radiation. In the low-temperature experiment, the crystal cooling was achieved by a cold nitrogen gas flow surrounded by a jacket of dry nitrogen gas at room temperature to prevent frost from growing around the sample. At $T \approx 130$ K, the temperature fluctuation is assumed to be about ±2 K. The crystal was a black plate-shaped single crystal of size 0.07 × 0.20 × 0.20 mm.

Table I. Crystal Data and Conditions for Crystallographic Data Collection and Structure Refinement

	$T \simeq 293$ K	$T \simeq 130$ K
formula	$C_{26}H_{16}N_6S_2Fe$	
fw	532.4	
cryst syst	orthorhombic	
space group	*Pbcn* (D_{2h}^{14})	*Pbcn* (D_{2h}^{14})
a, Å	13.1612 (18)	12.7699 (21)
b, Å	10.1633 (11)	10.0904 (25)
c, Å	17.4806 (19)	17.2218 (30)
V, Å^3	2338.2	2219.0
D(calcd), g·cm^{-3}	1.512	1.593
Z	4	
λ(Mo Kα), Å	0.71069	
μ(Mo Kα), cm^{-1}	8.637	
diffractometer	NONIUS CAD-4	
unit cell	25 reflcns ($5 \le \theta \le 15°$)	
scan type	$\omega/2\theta$	
scan width, deg	$1.6 + 0.35 \tan \theta$	
θ range, deg	1–26	
no. of measd reflcns	1736	1814
no. of obsd reflcns $F_o^2 > 2\sigma(F_o)^2$	1050	1115
determination program	MITHRIL	
refinement program	SHELX 76	
no. of refined params	167	
minimized function	$\sum w\|\|F_o\| - \|F_c\|\|^2$	
weighting scheme	$w = 1/[\sigma^2(F_o) + gF_o^2]$	
g	0.00011	0.00059
R	0.034	0.041
R_w	0.032	0.039
max peak in final ($\Delta\rho$), e·Å^{-3}	0.5	0.6

Details on crystal data, data collections, and structure refinements are summarized in Table I. Lattice parameters were obtained from a least-squares refinement of the setting angles of 25 reflections in the $5 \le \theta \le 15°$ range. The intensities of 1736 ($T \approx 293$ K) and 1814 ($T \approx 130$ K) independent Bragg reflections ($1 \le \theta \le 26°$; $h_{max} = 12$, $k_{max} = 15$, $l_{max} = 20$) were collected by $\omega/2\theta$ scans. Lorentz polarization and absorption corrections were applied. 1050 ($T \approx 293$ K) and 1115 ($T \approx 130$ K) reflections for which $F_o^2 > 2\sigma(F_o)^2$ were used to refine the structure.

At room temperature, the positions of Fe and S atoms were deduced from a Patterson synthesis, and the complete structure was solved by Fourier recycling, using the program MITHRIL.[33] The final atomic coordinates were used as starting values in the low-temperature refinement. The full-matrix refinement, based on F_o, was carried out using the program SHELX 76.[34] Atomic scattering factors were taken from ref 35. Final refinement minimizing $\sum w(|F_o| - |F_c|)^2$ converge at $T \approx 293$ K to $R = \sum||F_o| - |F_c||/\sum|F_o| = 0.034$ (0.041 at $T \approx 130$ K) and $R_w = \sum w^{1/2}||F_o| - |F_c||/\sum w^{1/2}|F_o| = 0.032$ (0.039 at $T \approx 130$ K). Non-hydrogen atoms were refined anisotropically. Fractional atomic coordinates and equivalent isotropic thermal parameters are given in Table II for $T \approx 293$ and $T \approx 130$ K.

It should be noted that the data collected at $T \approx 130$ K have been interpreted in terms of an "average" structure, described in the following, assuming all units in a low-spin configuration. In fact, attempts to refine a model of "semirigid" groups[36,37] in which the molar fractions of low- and high-spin forms are 0.83 and 0.17, respectively, (values estimated from magnetism experiments; vide infra) failed, as the final refined parameters were found unaltered compared to those obtained in the "average" structure.

Results

A. Magnetic Behavior. Magnetic susceptibility measurements were performed, first at decreasing then at increasing temperatures, on a polycrystalline sample prepared as described in the Experimental Section. The curve $\chi_m T$ vs T obtained in the

(28) Qi, Y.; Müller, E. W.; Spiering, H.; Gütlich, P. *Chem. Phys. Lett.* **1983**, *101*, 503.
(29) Rao, P. S.; Reuveni, A.; McGarvey, B. R.; Ganguli, P.; Gütlich, P. *Inorg. Chem.* **1981**, *20*, 204.
(30) Ganguli, P.; Gütlich, P.; Müller, E. W. *Inorg. Chem.* **1982**, *21*, 3429.
(31) Purcell, K. F.; Edwards, M. P. *Inorg. Chem.* **1984**, *23*, 2620.
(32) Spacu, P.; Teodorescu, M.; Lepadata, C. *Rev. Roum. Chim.* **1967**, *12*, 145; id. *Monatsh. Chem.* **1972**, *103*, 1.
(33) Gilmore, C. J. *J. Appl. Crystallogr.* **1984**, *17*, 42.
(34) Sheldrick, G. M. *SHELX 76 System of Computing Programs*; University of Cambridge: Cambridge, England 1976.
(35) *International Tables for X-ray Crystallography*; Kynoch Press: Birmingham, England 1974; Vol. 4, p 99.
(36) Katz, B. A.; Strouse, C. E. *J. Am. Chem. Soc.* **1979**, *101*, 6214.
(37) Scheidt, W. R.; Geiger, D. K.; Haller, K. J. *J. Am. Chem. Soc.* **1982**, *104*, 495.

Table II. Atomic Coordinates ($\times 10^4$) and Isotropic Thermal Parameters (Å^2) for Non-Hydrogen Atoms

	x/a	*y/b*	*z/c*	U_{eq}[a]
		$T \simeq 293$ K		
Fe	0	6629 (1)	2500	498
N(1)	−1608 (2)	6256 (3)	2762 (2)	534
N(2)	50 (3)	5076 (3)	3386 (2)	558
N(20)	413 (3)	7998 (4)	3309 (2)	695
C(1)	−1766 (3)	5285 (4)	3289 (2)	524
C(2)	−898 (4)	4682 (4)	3620 (2)	535
C(3)	−2412 (3)	6843 (4)	2443 (3)	638
C(4)	−3413 (3)	6504 (5)	2628 (3)	744
C(5)	−3574 (3)	5525 (5)	3161 (3)	745
C(6)	−2746 (3)	4895 (4)	3504 (2)	605
C(7)	−2855 (4)	3883 (5)	4065 (3)	797
C(8)	−2034 (4)	3289 (5)	4386 (3)	810
C(9)	−1021 (3)	3694 (5)	4178 (3)	689
C(10)	−150 (4)	3117 (5)	4498 (3)	876
C(11)	783 (4)	3560 (5)	4276 (5)	923
C(12)	858 (4)	4547 (5)	3720 (3)	726
C(21)	827 (3)	8731 (5)	3708 (3)	620
S(22)	1400 (1)	9761 (1)	4276 (1)	855
		$T \simeq 130$ K		
Fe	0	6447 (1)	2500	295
N(1)	−1531 (3)	6287 (3)	2764 (2)	285
N(2)	119 (3)	5067 (4)	3333 (2)	206
N(20)	302 (3)	7811 (4)	3276 (3)	382
C(1)	−1719 (4)	5336 (5)	3301 (3)	299
C(2)	−825 (4)	4677 (5)	3618 (3)	341
C(3)	−2354 (4)	6909 (4)	2454 (3)	356
C(4)	−3378 (4)	6605 (5)	2662 (3)	442
C(5)	−3583 (4)	5652 (5)	3204 (3)	431
C(6)	−2730 (4)	4973 (5)	3548 (3)	361
C(7)	−2827 (4)	3955 (5)	4119 (3)	439
C(8)	−1972 (5)	3368 (5)	4430 (3)	469
C(9)	−944 (4)	3732 (5)	4194 (3)	396
C(10)	−39 (5)	3143 (5)	4495 (3)	503
C(11)	919 (4)	3572 (5)	4235 (4)	468
C(12)	972 (4)	4530 (5)	3647 (3)	418
C(21)	686 (4)	8580 (5)	3670 (3)	323
S(22)	1249 (1)	9683 (1)	4233 (1)	448

[a] Values for anisotropically refined atoms are given in the form of the isotropic equivalent thermal parameter $U_{eq} = {}^1/_3(U_{11} + U_{22} + U_{33})$.

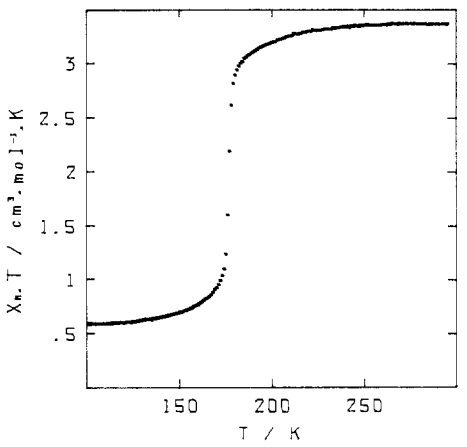

Figure 1. Temperature dependence of $\chi_m T$ for a polycrystalline sample of $Fe(phen)_2(NCS)_2$ prepared as described in the Experimental Section (the curves obtained at decreasing and increasing temperatures being hardly distinguishable, only the former is represented for clarity).

warming up mode is shown in Figure 1. It is quite similar to that obtained in the cooling mode.

As indicated by the data, the possible hysteresis cannot be wider than about 1 K, which is in keeping with the results reported by Müller et al.[10] The $\chi_m T$ product decreases slightly from 3.41 cm^3·mol^{-1}·K at 292 K to 2.83 cm^3·mol^{-1}·K at 178 K (μ_{eff} = 5.22 to 4.75 μB), then drops suddenly around $T_c \approx 176.5$ K down to 1.04 cm^3·mol^{-1}·K (μ_{eff} = 2.88 μB) at 173 K, and reaches the lower limit of 0.58 cm^3·mol^{-1}·K (μ_{eff} = 2.16 μB) in the vicinity of 110 K. This last value shows that the transition is not complete at low temperature; the proportion of molecules that are retained in the high-spin form can be estimated to be ≈17%.

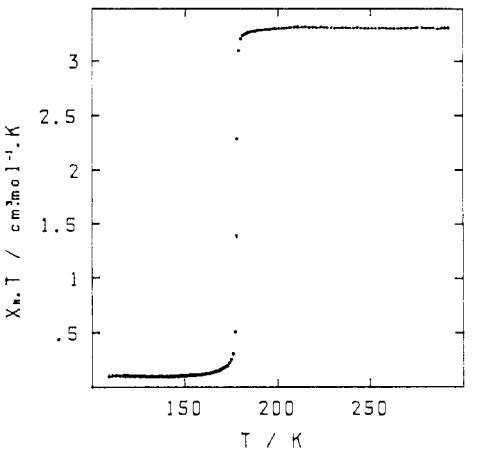

Figure 2. Temperature dependence of $\chi_m T$ for a sample of $Fe(phen)_2(NCS)_2$ prepared by the "extraction" method[5] (the curves obtained at decreasing and increasing temperatures being hardly distinguishable, only the former is represented for clarity).

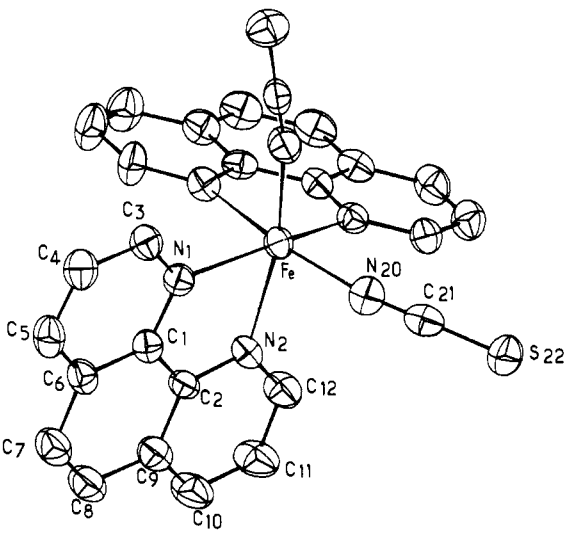

Figure 3. Drawing of the $Fe(phen)_2(NCS)_2$ unit, showing the 50% probability ellipsoids at $T \approx 293$ K. Hydrogen atoms have been omitted for clarity.

It is clear that the magnetic behavior of this polycrystalline sample is different from the typical one we observed for a powder obtained by the extraction method (see Figure 2). On the other hand, it closely resembles that reported for powder samples prepared by precipitation.[5,9,10]

B. Description of the Structures. No evidence has been provided for a change in the space group over the 293–130 K temperature range. The arrangement of $Fe(phen)_2(NCS)_2$ units is quite the same in the low- and high-spin forms, the most remarkable differences being observed in the intramolecular geometry of the complex. Figure 3 shows a perspective drawing of the molecule together with the numbering of the atoms included in the asymmetric unit. Each iron atom is surrounded by six nitrogen atoms belonging to two $(NCS)^-$ groups in cis positions and two 1,10-phenanthroline ligands. It follows that the molecule is chiral and that each unit cell contains two right-handed and two left-handed enantiomers. Interatomic distances and bond angles related to the high-spin ($T \approx 293$ K) and low-spin ($T \approx 130$ K) isomers are listed in Tables III and IV.

High-Spin-Form Structure ($T \approx 293$ K). The phenanthroline ligands are nearly planar. If the least-squares plane of each ligand (equation: $-0.0016X + 0.6893Y + 0.7244Z = 7.8714$ Å) is defined by the positions of the central ring carbon atoms (C(1), C(2), C(6), C(7), C(8), C(9)), the largest deviation is found to

Table III. Bond Lengths (in Å)[a]

	$T \simeq 293$ K	$T \simeq 130$ K
N(1)–Fe	2.199 (3)	2.014 (4)
N(2)–Fe	2.213 (3)	2.005 (4)
N(20)–Fe	2.057 (4)	1.958 (4)
C(1)–N(1)	1.366 (4)	1.355 (5)
C(3)–N(1)	1.337 (4)	1.335 (6)
C(2)–N(2)	1.373 (4)	1.361 (6)
C(12)–N(2)	1.327 (4)	1.331 (6)
C(21)–N(20)	1.158 (4)	1.140 (6)
C(2)–C(1)	1.421 (5)	1.429 (6)
C(6)–C(1)	1.401 (5)	1.407 (6)
C(9)–C(2)	1.408 (5)	1.385 (6)
C(3)–C(4)	1.399 (5)	1.390 (7)
C(4)–C(5)	1.380 (5)	1.365 (6)
C(5)–C(6)	1.399 (5)	1.416 (6)
C(7)–C(6)	1.428 (5)	1.428 (6)
C(8)–C(7)	1.359 (6)	1.353 (7)
C(9)–C(8)	1.442 (5)	1.422 (7)
C(10)–C(9)	1.404 (5)	1.399 (7)
C(11)–C(10)	1.364 (5)	1.374 (7)
C(12)–C(11)	1.400 (5)	1.401 (7)
S(22)–C(21)	1.628 (5)	1.632 (4)

[a] Numbers in parentheses are estimated standard deviations in the least significant digit.

Table IV. Bond Angles (in deg)[a]

	$T \simeq 293$ K	$T \simeq 130$ K
N(2)–Fe–N(1)	76.1 (1)	81.8 (1)
N(20)–Fe–N(1)	103.2 (1)	95.3 (1)
N(20)–Fe–N(2)	89.6 (1)	89.1 (1)
C(1)–N(1)–Fe	114.3 (2)	112.5 (3)
C(3)–N(1)–Fe	126.7 (3)	129.5 (3)
C(3)–N(1)–C(1)	118.9 (3)	117.8 (4)
C(2)–N(2)–Fe	113.0 (3)	113.1 (3)
C(12)–N(2)–Fe	128.4 (3)	129.5 (3)
C(12)–N(2)–C(2)	118.6 (3)	117.4 (4)
C(21)–N(20)–Fe	167.0 (4)	165.6 (4)
C(2)–C(1)–N(1)	117.7 (4)	116.6 (4)
C(6)–C(1)–N(1)	121.8 (4)	123.6 (4)
C(6)–C(1)–C(2)	120.6 (4)	119.7 (4)
C(1)–C(2)–N(2)	118.9 (4)	115.9 (4)
C(9)–C(2)–N(2)	121.3 (4)	123.7 (5)
C(9)–C(2)–C(1)	119.8 (4)	120.4 (5)
C(5)–C(6)–C(1)	118.2 (4)	116.9 (4)
C(7)–C(6)–C(1)	118.7 (4)	118.4 (4)
C(7)–C(6)–C(5)	123.1 (4)	124.7 (4)
C(4)–C(5)–C(6)	120.0 (4)	118.6 (5)
C(5)–C(4)–C(3)	118.6 (4)	120.8 (5)
C(4)–C(3)–N(1)	122.6 (4)	122.2 (5)
C(8)–C(7)–C(6)	121.6 (4)	121.2 (5)
C(9)–C(8)–C(7)	120.2 (5)	121.3 (5)
C(8)–C(9)–C(2)	119.0 (4)	118.9 (5)
C(10)–C(9)–C(2)	118.6 (4)	117.9 (5)
C(11)–C(10)–C(9)	118.9 (4)	118.8 (4)
C(12)–C(11)–C(10)	119.8 (5)	119.7 (5)
C(11)–C(12)–N(2)	122.6 (4)	122.4 (5)
S(22)–C(21)–N(20)	179.4 (4)	179.5 (4)

[a] Numbers in parentheses are estimated standard deviations in the least significant digit.

be 0.036 Å. The angle between the two phenanthroline planes in a given molecule is 92.85°.

Whereas the $(NCS)^-$ groups are linear (N(20)–C(21)–S(22) = 179.4 (4)°), the Fe–N–C(S) linkages are bent (Fe–N(20)–C(21) = 167.0 (4)°). The involved Fe–N distances (Fe–N(20) = 2.057 (4) Å) are shorter than those of the Fe–N(phen) bonds (mean value = 2.206 Å). This leads to a strong distorsion of the $[Fe–N_6]$ octahedron, which is well illustrated by the differences in the N–Fe–N angles:

$$N(1)–Fe–N(2) = 76.1\ (1)°$$

$$N(20)–Fe–N(1) = 103.2\ (1)°$$

$$N(20)–Fe–N(2) = 89.6\ (1)°$$

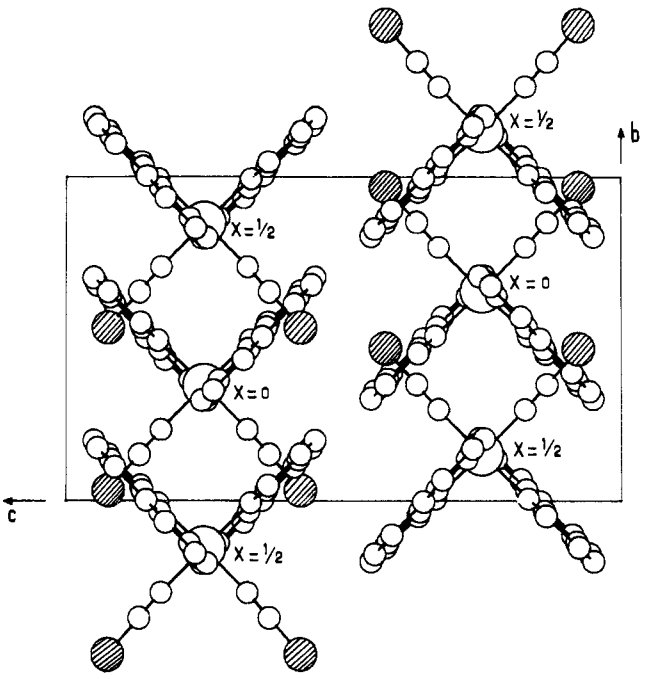

Figure 4. Projection of the molecular structure along the *a* axis.

Table V. Intermolecular Distances (Å) Shorter at $T \simeq 130$ K Than the van der Waals Distances and Fe···Fe Distances Involved in the Same Interactions[a]

	$T \simeq 293$ K	$T \simeq 130$ K
$S(22)–C(7)_{i}$	3.357 (5)	3.367 (5)
$C(7)–S(22)_{i'}$	3.357 (5)	3.367 (5)
$C(4)–C(9)_{ii}$	3.584 (5)	3.510 (7)
$C(9)–C(4)_{ii'}$	3.584 (5)	3.510 (7)
$C(3)–C(7)_{ii}$	3.531 (6)	3.541 (7)
$C(7)–C(3)_{ii'}$	3.531 (6)	3.541 (7)
$C(5)–C(8)_{ii}$	3.622 (7)	3.531 (8)
$C(8)–C(5)_{ii'}$	3.622 (7)	3.531 (8)
$C(5)–C(9)_{ii}$	3.717 (7)	3.596 (7)
$C(9)–C(5)_{ii'}$	3.717 (7)	3.596 (7)
$C(4)–C(8)_{ii}$	3.617 (7)	3.555 (8)
$C(8)–C(4)_{ii'}$	3.617 (7)	3.555 (8)
$C(21)–C(5)_{ii}$	3.610 (7)	3.497 (7)
$C(5)–C(21)_{ii'}$	3.610 (7)	3.497 (7)
$Fe···Fe_{i}$	11.083 (6)	10.928 (6)
$Fe···Fe_{i'}$	11.083 (6)	10.928 (6)
$Fe···Fe_{ii}$	8.314 (6)	8.138 (6)
$Fe···Fe_{ii'}$	8.314 (6)	8.138 (6)

[a] The first mentioned atom is related to a given central *x*, *y*, *z* molecule. Small characters in subscript give the symmetry operation and the associated translations for the second atom involved in a considered interaction:

i	$^1/_2 + x, {}^1/_2 - y, -z$	$\bar{1}11$
i′	$^1/_2 + x, {}^1/_2 - y, -z$	011
ii	$^1/_2 - x, {}^1/_2 + y, z$	$\bar{1}00$
ii′	$^1/_2 - x, {}^1/_2 + y, z$	$\bar{1}\bar{1}0$

Figure 4 shows a projection of the structure along the *a* axis. The molecular packing may be described as sheets of complex molecules parallel to the *a*–*b* plane, in which adjacent units, located by the position of their central Fe atom, alternate along the *b* direction at the coordinates $x = 0$ and $x = {}^1/_2$.

The cohesion of the structure is achieved by van der Waals interactions. Within a sheet, the shortest distances (see Table V) are only observed between the carbon atoms of the phenanthroline groups $(C(3)–C(7)_{ii} = 3.531\ (6)$ Å; $C(4)–C(9)_{ii} = 3.584\ (5)$ Å) while, if one considers the interactions between consecutive sheets, S–C contacts appear to be the only appreciable ones $(S–C(7)_{i} = 3.357\ (5)$ Å).

Low-Spin-Form Structure ($T \approx 130$ K). At low temperature, the more noticeable intramolecular modifications associated with

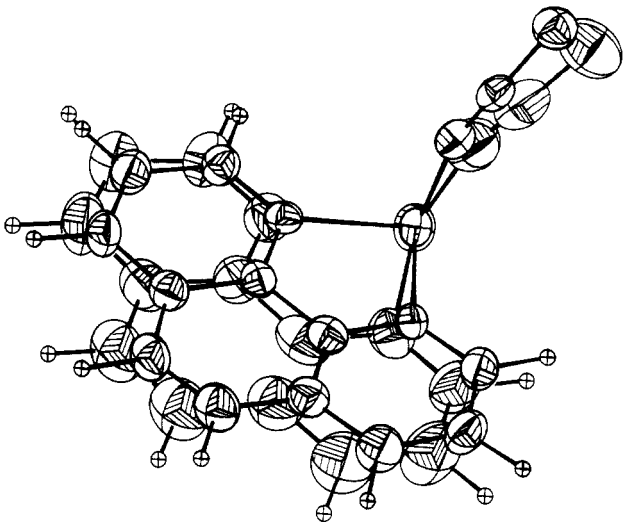

Figure 5. Schematic drawing of both high-spin ($T \approx 293$ K) and low-spin ($T \approx 130$ K) isomers. The asymmetric unit at $T \approx 130$ K is the upper one. Fe–N(1) bonds are superimposed.

the spin transition are those that affect the [Fe–N_6] core geometry.

The high-spin → low-spin conversion is characterized by a shortening of the Fe–N distances, which depends on the nitrogen atom involved in the bonds. In the low-spin isomer, Fe–N(phen) bonds are shorter by about 0.20 Å compared to those in the high-spin isomer (see Table III), while the Fe–N(CS) shortening is only 0.10 Å. It follows that the differences noted in Fe–N bond lengths at room temperature (2.20, 2.21, and 2.06 Å) significantly decrease at low temperature (2.01, 2.00, and 1.96 Å).

The $S = 2 \rightarrow S = 0$ spin change is also characterized by a variation of the N–Fe–N bond angles, which are approaching 90°. This fact is clearly established (see Table IV), particularly when examining the variations (+6° and −8°, respectively) of the N(2)–Fe–N(1) and N(20)–Fe–N(1) angles, the values of which strongly differ from 90° in the high-spin form.

Nevertheless, the general conformation of the complex is nearly unchanged upon cooling.

No significant differences are noted (see Tables III and IV) in bond lengths and angles for the phenanthroline units. These latter remain planar without noticeable variations in atomic shifts from the least squares plane. At $T \approx 130$ K (equation of the least-squares plane: $0.0388X + 0.6979Y + 0.7151Z = 7.7298$ Å), the largest shift is 0.041 Å instead of 0.036 Å in the high-spin state. Besides, the angle between the two phenanthroline planes (91.5°) is close to its room-temperature value (92.8°).

The shortening of the Fe–N distances does not affect the linearity of the $(NCS)^-$ groups. Moreover, these groups remain similarly bent with regard to the Fe–N(CS) bonds over the whole temperature range, the small variation of the Fe–N(20)–C(21) angle being insignificant.

Figure 5 shows two projections of the asymmetric unit onto its mean plane, at ≈293 and ≈130 K, respectively, keeping the Fe atomic position and the Fe–N(1) direction unchanged; the thermal ellipsoids derived from the ≈130 K data are, for each atom, the upper ones. The figure clearly shows the previously described modifications in the intramolecular geometry when passing from the high- to the low-spin form, i.e. the shortening of Fe–N distances and the noticeable variation of N–Fe–N angles, leading to a more regular shape of the [FeN_6] octahedron. Qualitative differences in the atomic temperature factors can also be observed.

Intermolecular distances shorter than the van der Waals contacts at ≈130 K, as well as Fe···Fe distances between the molecules involved in these interactions, are reported in Table V. A close examination of the data reveals that the C···C intermolecular contacts (<3.60 Å) are less numerous at room temperature than at 130 K and that the S···C ones (<3.85 Å) remain the only interactions between consecutive sheets in the *c* direction. It should be noted that the variations in intermolecular contacts are driven by both the thermal contraction of lattice parameters over the whole temperature range and the strengthening of metal–ligand bonds upon the spin transition. The shortening of the Fe···Fe distances only results from the thermal contraction, whereas a consequence of the strengthening of metal–ligand bonds is to reduce the C···C and C···S contacts between ligands of adjacent molecules and thus to lower the effects of thermal contraction on these distances. This may explain why the average shortening of C···C and C···S intermolecular distances, when the temperature decreases from ≈293 to ≈130 K, is less important than that of Fe···Fe intervals.

Table VI. Room-Temperature Crystal Data for $Fe(phen)_2(NCS)_2$ (This Work) and Polymorphs I and II of $Fe(bpy)_2(NCS)_2$[38]

	$Fe(phen)_2(NCS)_2$	$Fe(bpy)_2(NCS)_2$	
		polymorph I	polymorph II[a]
system	orthorhombic	orthorhombic	orthorhombic
space group	*Pbcn* (D_{2h}^{14})	*Pbca* (D_{2h}^{15})	*Pbcn* (D_{2h}^{14})
a, Å	13.1612 (18)	16.04 ± 0.05	13.17 ± 0.05
b, Å	10.1633 (11)	16.98 ± 0.05	10.08 ± 0.04
c, Å	17.4606 (19)	15.94 ± 0.05	16.50 ± 0.05
Z	4	8	4

[a] For comparison, the *Pcnb* space group reported by König et al.[38] was converted into *Pbcn*; so, the *b* and *c* axes defined by these authors were inverted.

Discussion

Polymorphs of $Fe(phen)_2(NCS)_2$. It is interesting to compare the above-mentioned magnetic and structural data relating to $Fe(phen)_2(NCS)_2$ with those reported for the parent complex $Fe(bpy)_2(NCS)_2$ (bpy = 2,2′-bipyridine).

The latter compound, which also exhibits a sharp spin transition (at ≈215 K), can exist in three crystalline forms, depending on the synthesis procedures.[38,39] A single-crystal X-ray analysis has been performed on polymorph I at 295 K[38] and on polymorph II at 295[38,40] and ≈100 K[40] (polymorph III could not be structurally characterized). The essential room-temperature crystal data of both forms and those obtained in the present work for $Fe(phen)_2(NCS)_2$ are listed in Table VI. It clearly appears that the characteristics of the phenanthroline derivative are very close to those of the polymorph II of $Fe(bpy)_2(NCS)_2$ (same space group and number of molecules per unit cell and similar values for *a*, *b*, and *c* parameters). The analogy presented by the two compounds is supported by some additional features: (i) the variations of the metal–ligand distances associated with the spin transition are about twice as large for the iron–N(heterocycle) bonds as for the iron–N(CS) bonds (0.185 and 0.208 Å for Fe–N(phen) and 0.099 Å for Fe–N(CS) in $Fe(phen)_2(NCS)_2$; 0.12 and 0.16 Å for Fe–N(bpy) and 0.08 Å for Fe–N(CS) in $Fe(bpy)_2(NCS)_2$, polymorph II[40]); (ii) the [FeN_6] core approximates O_h symmetry much more closely in the low-spin form than in the high-spin form;[40] (iii) the spin conversion is not complete at low temperature, the fraction of high-spin form retained in the low-spin form matrix being estimated at ≈17% for the phenanthroline derivative and ≈18% for the bipyridine one.[41]

From the above considerations, it follows that the $Fe(phen)_2(NCS)_2$ crystals investigated in the present work can be considered as "polymorph II" crystals, by analogy with $Fe(bpy)_2(NCS)_2$. Moreover, as the relevant μ_{eff} vs *T* curve is quite similar to the typical curve obtained with "precipitated" samples,[5,10] which has the same shape and very close upper (5.2–5.3 μB) and lower (2.15–2.40 μB) limits for μ_{eff}, the precipitation method is very likely to lead also to polymorph II. Consequently, the very sharp transitions exhibited by the "extracted" samples of $Fe(phen)_2(NCS)_2$, which are nearly complete at low temperature ($\mu_{eff} \approx 0.5$–0.9 μB; i.e., $\chi_m T \approx 0.03$–0.10 $cm^3 \cdot mol^{-1} \cdot K$)[5,10] (see Figure 2) and closely resemble those presented by the polymorph I of

(38) König, E.; Madeja, K.; Watson, K. J. *J. Am. Chem. Soc.* **1968**, *90*, 1146.
(39) Casey, A. T. *Aust. J. Chem.* **1968**, *21*, 2291.
(40) König, E.; Watson, K. J. *Chem. Phys. Lett.* **1970**, *6*, 457.
(41) König, E. *Prog. Inorg. Chem.* **1987**, *35*, 527.

$Fe(bpy)_2(NCS)_2$,[38] are certainly typical of another structural form we shall call polymorph I.

So, evidence seems provided for the existence, predicted by König,[38] of at least two polymorphs for $Fe(phen)_2(NCS)_2$. It follows that the differences in spin transition characteristics presented by "precipitated" and "extracted" samples must mainly arise from the fact that the structural form involved is not the same in the two cases. Sizes and principally defects of crystals, which have always been considered as entirely responsible for these differences,[9,10] are then expected to play only a secondary part: their influence would explain why samples, prepared independently but by the same method, do not quite present the same spin-crossover behavior. This conclusion is supported by the data reported by Müller et al.:[10] the μ_{eff} vs T curve of an "extracted" sample ground for 6 h in a ball mill resembles much more the curve obtained with the unperturbed "extracted" sample than that corresponding to a "precipitated" one.

Structural Changes upon the Spin Transition. Let us now consider the changes in molecular structure associated with the spin transition.

The most conspicuous variations concern the metal–ligand bond lengths. In the present case, the mean value of this variation, $\overline{\Delta R}$, is found to be 0.164 Å. This value lies in the range 0.19 ± 0.05 Å defined for $S = 0 \leftrightarrow S = 2$ conversions in the iron(II) spin-crossover compounds having a $[FeN_6]$ coordination core.[41-43] $\overline{\Delta R}$ is known to influence the transition characteristics. Indeed, it seems now well established that the cooperative nature of a discontinuous spin transition arises from significant coupling between the electronic states of the metal ion and the lattice phonon system through metal–ligand vibrations and, consequently, that the phenomenon proceeds via the formation of domains constituted of like-spin molecules. The stronger the coupling, particularly the more important the variation of the coordination core vibrational frequencies (hence the metal–ligand bond length changes) upon the spin conversion, the sharper the transition. The latter part of this statement can be corroborated if one takes into account the existence of at least two polymorphs for $Fe(phen)_2(NCS)_2$. Indeed, the $\overline{\Delta R}$ value (0.164 Å) obtained for polymorph II is actually found to be much lower than that (0.24 Å) deduced from EXAFS experiments on an "extracted" sample[18] (polymorph I), the transition of which is much more abrupt than that of polymorph II (see Figure 2).

The larger decrease observed for Fe–N(phen) distances ($\Delta R \approx 0.2$ Å) as compared with Fe–N(CS) distances ($\Delta R \approx 0.1$ Å), when passing from the high- to the low-spin form, may be mainly accounted for by the fact that the 1,10-phenanthroline acts as a much stronger π-electron acceptor than the $(NCS)^-$ group. In the low-spin isomer, the electron back-donation from filled metal π orbitals (t_{2g} orbitals in the O_h approximation) to vacant π^* ligand orbitals is, therefore, expected to be much more important for 1,10-phenanthroline than for $(NCS)^-$, which results in a higher strengthening of Fe–N(phen) with regard to Fe–N(CS) bonds.

A length decrease, from 1.158 (4) to 1.140 (6) Å, is observed for N–C(S) bonds on going from ≈293 to ≈130 K. By contrast, in the case of polymorph II of $Fe(bpy)_2(NCS)_2$, an increase of the N–C(S) distances from 1.08 (4) Å at 293 K to 1.16 (4) Å at ≈105 K was reported.[40] So, upon the spin-state transition, the N–C(S) bonds are found to be slightly strengthened in the phenanthroline compound and significantly loosened in the bipyridine compound. A possible explanation for this difference in behavior is that, in the low-spin form, the metal → $(NCS)^-$ π-back-donation, which reduces the N–C(S) bond strength, is much weaker in $Fe(phen)_2(NCS)_2$ than in $Fe(bpy)_2(NCS)_2$, as a consequence of the higher t_{2g} electron deficiency at the iron atom caused by the stronger metal → heterocycle π-back-donation. However, it is surprising to note that, in both cases, similar shifts of ν(C–N(S)) asymmetric and symmetric stretching modes toward higher frequencies were observed (from 2075 and 2063 cm^{-1} to 2116 and 2108 cm^{-1} for $Fe(phen)_2(NCS)_2$;[3,5,13] from 2065 and 2055 cm^{-1} to 2109 and 2100 cm^{-1} for $Fe(bpy)_2(NCS)_2$ polymorph II[38]). Such shifts (40–45 cm^{-1}) are in keeping with the shortening of the N–C(S) bond in the phenanthroline compound.

At least, it should be emphasized that the spin-state transition does not affect the linearity of $(NCS)^-$ groups and has little influence on Fe–N–C(S) angles. Concerning these angles, it seems interesting to compare the values found in the present work (167.0° at ≈293 K; 165.6° at ≈130 K) to those reported for $[Fe(bpym)(NCS)_2]_2bpym$ (158.2 and 172.2°)[44] and $Fe(bt)_2(NCS)_2$ (163.3 and 178.1° in polymorph A; 160.4° and 159.8° in polymorph B),[45] "bpym" being 2,2′-bipyrimidine and "bt" being 2,2′-bi-2-thiazoline.

Mechanism of the Spin Transition. Despite the large number of available experimental data, all the factors governing the discontinuous $S = 0 \leftrightarrow S = 2$ spin transition presented by $Fe(phen)_2(NCS)_2$ are not yet well specified.

The polymorph II structures described in this paper show that, in disagreement with most of the predictions, the transition is neither associated with a change in the crystal symmetry (as already observed in the quasi-totality of the multitemperature structural studies of the spin-crossover compounds reported up to now[41]) nor triggered by a structural order–disorder transition involving the $(NCS)^-$ groups that would occupy different rotational positions in the high-temperature range. Only a large rearrangement of the iron atom environment is detected. This is in agreement with the conclusion deduced by Rao et al. from the ESR study of a "precipitated" sample of $Fe(phen)_2(NCS)_2$ doped with manganese(II):[29] the fact that the temperature dependence of D and E parameters was found not to be affected by the transition led these authors to state that the structural changes associated with the spin conversion were short-range ones inside the complex and not long-range ones involving the total lattice.

Moreover, the values found for the mean variation of the metal–ligand bond lengths (0.164 Å) and for the change of the unit cell volume (≈5%, i.e. ≈30 $Å^3$ per iron atom) cannot account for the first-order character of the transition, evidenced by the temperature dependence of $\chi_m T$ (see Figure 1), the existence of a significant latent heat,[9] and the existence of a hysteresis effect (of 1.5 (5) K).[10] Indeed, these values are very close to those reported for some spin-crossover mononuclear iron(II) complexes with $[FeN_6]$ coordination cores, which have the same order of magnitude whether the transition is discontinuous or continuous ($\Delta V/V \approx 3.8$–6.0%, $\Delta V \approx 25$–35 $Å^3$ per iron atom, $\overline{\Delta R} = 0.19 \pm 0.05$ Å).[18,41-43]

So, the main structural feature relating to the sharpness of the spin transition of $Fe(phen)_2(NCS)_2$ (polymorph II) seems to be the reorganization of $[FeN_6]$ octahedrons toward a more regular shape when passing from the high- to the low-spin form, and conversely. A higher symmetry at the metal center would be associated with a change in the electronic configuration, the low-symmetry splitting of the $^5T_2$ state, at the origin of the high-spin ground state, being reduced in such a way that a $^1A_1$ low-spin ground state would result. A similar hypothesis was suggested by König and Ritter in the case of $Fe(bpy)_2(NCS)_2$.[46] It may be assumed that the rather strong cooperativity of the spin transition arises from the conjunction of the spin conversion with this structural change of the coordination core.

As seen above, the high-spin to low-spin conversion of the $Fe(phen)_2(NCS)_2$ polymorph II does not proceed to completion at low temperature (see Figure 1). The lower cooperativity of this transition, as compared with that observed for polymorph I (whose transition is nearly complete at both increasing and decreasing temperatures (see Figure 2)), is likely to play a large part in the incompleteness process. Indeed, many domains are then

(42) Thuéry, P.; Zarembowitch, J.; Michalowicz, A.; Kahn, O. *Inorg. Chem.* **1987**, *26*, 851.
(43) Baker, A. T.; Goodwin, H. A.; Rae, A. D. *Inorg. Chem.* **1987**, *26*, 3513.
(44) Real, J. A.; Zarembowitch, J.; Kahn, O.; Solans, X. *Inorg. Chem.* **1987**, *26*, 2939.
(45) Ozarowski, A.; McGarvey, B. R.; Sarkar, A. B.; Drake, J. E. *Inorg. Chem.* **1988**, *27*, 628.
(46) König, E.; Ritter, G. *Phys. Lett.* **1973**, *43A*, 488.

expected not to grow large enough to remain in the low-spin state below the critical temperature and, therefore, to turn back to the high-spin state.

Additional single-crystal experiments are in progress to specify the mechanism of this spin transition, viz., (i) accurate measurements of the temperature dependence of the lattice parameters, to get further information about the correlation between the spin change and the structural reorganization, and (ii) determination of the compressibility tensor, with the purpose of investigating the electron–phonon coupling.

Supplementary Material Available: Tables of calculated fractional positions and isotropic thermal parameters for hydrogen atoms and anisotropic thermal parameters for non-hydrogen atoms (2 pages); tables of observed and calculated structure factors at room temperature and 130 K (14 pages). Ordering information is given on any current masthead page.

Contribution from the Department of Chemistry and Biochemistry, University of California, Los Angeles, California 90024

Excited-State Raman Spectroscopy of $W(CO)_4(\alpha\text{-diimine})$ Complexes

Jing-Huei Perng and Jeffrey I. Zink*

Received April 26, 1989

The Raman spectra of $W(CO)_4$(diimine) complexes (diimine = 2,2′-bipyridine, 4,4′-dimethyl-2,2′-bipyridine, and pyridine-2-carbaldehyde isopropylimine) in the lowest tungsten to diimine charge-transfer excited state are reported. The excited-state peaks are assigned to ligand ring deformation modes and to carbonyl stretching modes. The effect of the electron transfer on 2,2′-bipyridine and 4,4′-dimethyl-2,2′-bipyridine ring mode frequencies is similar to that previously observed on the prototypical ruthenium compounds. The totally symmetric cis-carbonyl stretching mode in the charge-transfer excited state is about 50 cm^{-1} higher in energy than that of the molecule in the ground electronic state. The increase is interpreted in terms of loss of metal–carbonyl π back-bonding in the charge-transfer excited state.

Raman spectroscopy of excited electronic states of transition-metal compounds is attracting increasing interest. Following the pioneering work of Woodruff and Dallinger,[1,2] a variety of metal complexes have been studied.[3-15] The primary area of interest has been the effect of the transfer of an electron to a ligand on the normal modes of the recipient ligand. More recently, several studies have probed the effect of electron transfer to a given ligand on the vibrational properties of other ligands in the molecule.[11,15] The latter area is the focus of this study.

A series of $W(CO)_4L$ complexes (L = diimine) were chosen for this study. The excited-state properties of these compounds have been studied both spectroscopically and photochemically by Oskam and co-workers.[16-20] These complexes have a low-lying metal-to-ligand charge-transfer transition in the visible region of the spectrum. The properties of the charge-transfer excited state were correlated with the energy of the π^* diimine ligand orbital. The higher the energy of the π^* orbital, the larger the solvatochromism and the larger the intensity of the resonance Raman band for the cis-CO and the CN normal modes.

In this paper, we report the Raman spectra of a series of $W(CO)_4(\alpha\text{-diimine})$ complexes in their metal-to-diimine charge-transfer excited states. Excited-state spectra were found for the complexes containing the 2,2′-bipyridine (bpy), 4,4′-dimethyl-2,2′-bipyridine (Me_2bpy), and pyridine-2-carbaldehyde isopropylimine (pyca) ligands. The structure of the latter ligand is shown below.

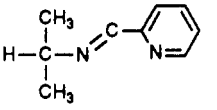

Excited-state Raman spectra in the 900–1600-cm^{-1} diimine ligand ring deformation region and in the CO stretching region are reported. The carbonyl bonding changes caused by the electron-transfer transition to the diimine ligands are discussed.

Experimental Section

The excited-state Raman spectra of the title complexes were obtained by exciting and probing with 406-nm, 10-ns pulses (0.4–2.0 mJ/pulse) at a 45-Hz repetition rate from an excimer pumped dye laser (Lambda Physik EMG 201 MSC and FL 2001). Dispersing prisms were used directly in front of the laser in order to reduce contributions from the background fluorescence from the dye laser. In addition, an iris diaphragm was used to block undesired frequencies from reaching the sample. The sample solutions ($\sim 1 \times 10^{-3}$ M) were prepared by dissolving the title complexes in CH_3CN. The room-temperature solution was circulated by a peristaltic pump through a 20-gauge hypodermic needle to produce a jet stream. The flow rate was about 0.3 mL/s. The laser beam was focused by using a plano-convex lens with 150-mm focal length. The focus was adjusted to lie about 5–8 mm behind the jet stream in order to minimize dielectric breakdown and the possibility of the stimulated Raman effect.[21,22] The Raman spectra were obtained by using a triple monochromator with an EG&G OMA III diode-array detector.

The ground-state Raman spectra of $W(CO)_4(Me_2bpy)$ were obtained by using argon ion laser excitation at 488 and 514.5 nm with 100–150 mW of power incident at a jet stream. The sample solutions ($\sim 10^{-3}$ M) were prepared by dissolving the complex in CH_3CN. The title com-

(1) Dallinger, R. F.; Woodruff, W. H. *J. Am. Chem. Soc.* **1979**, *101*, 4391.
(2) Bradley, P. G.; Kress, N.; Hornberger, B. A.; Dallinger, R. F.; Woodruff, W. H. *J. Am. Chem. Soc.* **1981**, *103*, 7441.
(3) Dallinger, R. F.; Miskowski, V. M.; Gray, H. B.; Woodruff, W. H. *J. Am. Chem. Soc.* **1981**, *103*, 1595.
(4) Forster, M.; Hester, R. E. *Chem. Phys. Lett.* **1981**, *81*, 42.
(5) Schindler, J. W.; Zink, J. I. *J. Am. Chem. Soc.* **1981**, *103*, 5968.
(6) Smothers, W. K.; Wrighton, M. S. *J. Am. Chem. Soc.* **1983**, *105*, 1067.
(7) McClanahan, S.; Hayes, T.; Kincaid, J. *J. Am. Chem. Soc.* **1983**, *105*, 4486.
(8) Chung, R. C.; Leventis, N.; Wagner, P. J.; Leroi, G. E. *J. Am. Chem. Soc.* **1985**, *107*, 1414.
(9) Chung, R. C.; Leventis, N.; Wagner, P. J.; Leroi, G. E. *J. Am. Chem. Soc.* **1985**, *107*, 1416.
(10) Dallinger, R. F. *J. Am. Chem. Soc.* **1985**, *107*, 7202.
(11) Yang, Y. Y.; Zink, J. I. *J. Am. Chem. Soc.* **1985**, *107*, 4799.
(12) McGarvey, J. J.; Bell, S. E. J.; Bechara, J. N. *Inorg. Chem.* **1986**, *25*, 4327.
(13) Bechara, J. N.; Bell, S. E. J.; McGarvey, J. J.; Rooney, J. J. *J. Chem. Soc., Chem. Commun.* **1986**, 1785.
(14) Mabrouk, P. A.; Wrighton, M. S. *Inorg. Chem.* **1986**, *25*, 526.
(15) Perng, J. H.; Zink, J. I. *Inorg. Chem.* **1988**, *27*, 1403.
(16) Balk, R. W.; Stufkens, D. J.; Oskam, A. *Inorg. Chim. Acta* **1979**, *34*, 267.
(17) Balk, R. W.; Snoeck, T.; Stufkens, D. J.; Oskam, A. *Inorg. Chem.* **1980**, *19*, 3015.
(18) Balk, R. W.; Stufkens, D. J.; Oskam, A. *J. Chem. Soc., Dalton Trans.* **1982**, 275.
(19) Servaas, P. C.; Van Dijk, H. K.; Snoeck, T. L.; Stufkens, D. J.; Oskam, A. *Inorg. Chem.* **1985**, *24*, 4494.
(20) Van Dijk, H. K.; Servaas, P. C.; Stufkens, D. J.; Oskam, A. *Inorg. Chim. Acta* **1985**, *104*, 179.
(21) Bloembergen, N. *Am. J. Phys.* **1967**, *35*, 989.
(22) Maier, M. *Appl. Phys.* **1976**, *11*, 209.

0020-1669/90/1329-1158$02.50/0